IET Nanobiotechnology

Special Issue: Selected Papers from The International Conference on Nanomaterials and Nanotechnology 2015

IET Journals
The Institution of Engineering and Technology

Synthesis and characterisation of PEG modified chitosan nanocapsules loaded with thymoquinone

ISSN 1751-8741
Received on 4th April 2016
Revised 20th October 2016
Accepted on 3rd November 2016
E-First on 15th December 2016
doi: 10.1049/iet-nbt.2016.0055
www.ietdl.org

Suresh Kumar Vignesh Kumar[1] ✉, Ponnuswamy Renuka Devi[1], Saru Harish[1], Eswaran Hemananthan[1]

[1]*Department of Biotechnology, Anna University Regional Campus, Coimbatore, Tamil Nadu, India*

✉ *E-mail: svigneshkum6@gmail.com*

Abstract: Thymoquinone (TQ), a major bioactive compound of *Nigella sativa* seeds has several therapeutic properties. The main drawback in bringing TQ to therapeutic application is that it has poor stability and bioavailability. Hence a suitable carrier is essential for TQ delivery. Recent studies indicate biodegradable polymers are potentially good carriers of bioactive compounds. In this study, polyethylene glycol (PEG) modified chitosan (Cs) nanocapsules were developed as a carrier for TQ. Aqueous soluble low molecular weight Cs and PEG was selected among different biodegradable polymers based on their biocompatibility and efficacy as a carrier. Optimisation of synthesis of nanocapsules was done based on particle size, PDI, encapsulation efficiency and process yield. A positive zeta potential value of +48 mV, indicating good stability was observed. Scanning electron microscope and atomic-force microscopy analysis revealed spherical shaped and smooth surfaced nanocapsules with size between 100 to 300 nm. The molecular dispersion of the TQ in Cs PEG nanocapsules was studied using X-ray powder diffraction. The Fourier transform infrared spectrum of optimised nanocapsule exhibited functional groups of both polymer and drug, confirming the presence of Cs, PEG and TQ. In vitro drug release studies showed that PEG modified Cs nanocapsules loaded with TQ had a slow and sustained release.

1 Introduction

Nigella sativa L. belongs to the Ranunculaceae family and grows in the Indian subcontinent and Mediterranean countries. The black seed of the plant was used from the ancient times in cooking and it was also referred as Habatul Baraka 'the Blessed Seed' [1]. *N. sativa* is being traditionally used in Ayurvedic medicine for more than 2000 years due to its anti-inflammatory property and anticancer activity through inhibition of the inflammatory pathway. *N. sativa* seed extract has been used by patients to suppress coughs, disintegrate renal calculi, impede the carcinogenic process, treat abdominal pain, diarrhea, flatulence and polio, exert choleretic and uricosuric activities [2, 3].

The principal bioactive component of *N. sativa* is thymoquinone (TQ) [1]. The other plants that contain TQ are *Callitris quadrivalvis, Monarda fistulosa, Juniperus* cedrus, *Tetraclinis articulata* and *Nepeta leucophylla* [4]. In past few decades, use of TQ as a pharmaceutical or nutraceutical agent is gaining a lot of importance in pharmaceutical and food formulations [5]. TQ is reported to have antioxidant, anti-inflammatory, anti-infective, neuroprotective, antiviral and anti-carcinogenic properties [6]. In the case of tumours, TQ reduces glutathione levels in a dose-dependent manner and induces reactive oxygen species generation. TQ is one of the rare bioactive compounds that can inhibit protein–protein interactions [6]. The anti-inflammatory property of TQ is by inhibition of cyclooxygenase and 5-lipoxygenase pathways of arachidonate metabolism. Antiapoptotic effect of TQ was reported by El-Khouly *et al.* [7]. The results of toxicity studies of fixed oil of *N. sativa* seeds indicated that *N. sativa* fixed oil has a low toxicity which was determined by its high LD50 values, key hepatic enzyme stability and organ integrity values [8]. The poor solubility and poor formulation characteristics of high lipophilic compound (TQ) limits its effectiveness and oral bioavailability [5]. Hence a suitable carrier is essential to encapsulate TQ and to increase its bioavailability.

The nature of carrier material [chitosan (Cs), cyclodextrins, PLGA etc.] has significant role on pharmacokinetics and pharmacodynamics of bioactive compounds. One of the important requirement in encapsulation system is to protect the bioactive component from chemical degradation (e.g. oxidation or hydrolysis) to keep the bioactive component fully functional. Polymer nanoparticles which are obtained from biodegradable and biocompatible polymers are good candidates for drug carrier to deliver drugs, because they are expected to be adsorbed in an intact form in the gastrointestinal tract after oral administration.

Chitosan is a cationic polyelectrolyte present in nature and is a co-polymer of glucosamine and N-acetylated glucosamine. It is derived from naturally occurring chitin by alkaline deacetylation. It is readily degraded into simple metabolising sugars and has good mucoadhesive and membrane permeability–enhancing properties [9]. The positive nature of chitosan serves for enhanced cellular interaction, delivery and increased penetration capacity in heterogeneous tumours [10]. The large number of free amine groups present in chitosan backbone when compared with other biodegradable polymers assists binding of many bioactive agents to the polymer [11]. Because of these reasons Cs has been extensively investigated for its potential as an absorption enhancer across intestinal epithelium for bioactive agents such as TQ. The one disadvantage of Cs is their solubility. However, it can overcome by preparing water soluble Cs [12]. Considering above mentioned advantages of Cs, it was chosen for encapsulating TQ efficiently. The high drug carrying capacity and longer shelf life of Cs compared with other biodegradable polymers [13, 14] also serves as an important factor for using chitosan as a nanocarrier in this study. Nanoparticles coated with Polyethylene glycol (PEG) have been found to be potential in the therapeutic application for controlled release of drugs and drug delivery to specific sites. PEG is non-toxic, non-immunogenic and commercially available Food and Drug Administration (FDA) USA approved polymer. PEG allows the slow release of drug from the capsules once it is attached to the capsules [15].

Considering the wide advantages of both Cs and PEG, there are few studies that have attempted to investigate PEGylated chitosan nanocapsules as an effective carrier. The incorporation of PEG in the gel system will be through the intermolecular hydrogen bonding between the electro-positive amino hydrogen of Cs and electronegative oxygen atom of PEG [16]. PEG modification has been proven to increase the systemic circulation lifetime and decrease the inflammatory responses by the body [17]. It reduces

the nanoparticle uptake by the reticuloendothelial system. Without PEG shell layer, aggregation of nanoparticles would take place in these organs and hence drug delivery would not be accomplished. Surface charge of polymeric drug carrier is hidden as PEG is non-ionic and hence less interaction with different blood components will occur, as a result opsonisation process can be reduced [18]. PEGylated lipid conjugated multidrug nanocapsules were reported to kill cancer cells effectively [19]. PEG is also believed to facilitate mucoadhession and consequent tansport through Peyer's patches of the GALT [20]. PEGylated chitosan has been successfully used for the encapsulating drugs such as methotrxate, mitomycin C, ormeloxifene etc. [10, 21–23]. The PEGylated chitosan nanocapsules are reported to exhibit dual role in both *invitro* and *invivo* studies [22, 24].

In interest to use the advantageous properties of both chitosan and PEG as a carrier, we studied and developed PEGylated water soluble Cs nanocapsules as a carrier for TQ. After wide literature survey, it was evident that no studies were reported on PEG modified water soluble Cs nanocapsules loaded with TQ for pharmaceutical and food applications.

2 Materials and methods

2.1 Materials

TQ was purchased from Sigma Aldrich, India. Cs was obtained from Central Institute of Fisheries Technology, Cochin, India. Polyethylene glycol (PEG: Molecular Weight – 4000) was purchased from Hi Media, India. All the other chemicals used are of analytical grade. Double distilled water was used throughout the work.

2.2 Methods

2.2.1 Preparation of aqueous soluble Cs (low molecular weight Cs): Acidic aqueous solution of Cs [25] was taken in a three-necked flat-bottomed flask and purged with nitrogen at 60°C while stirring at 200 rpm. Freshly prepared 0.8 mM of aqueous potassium persulfate ($K_2S_2O_8$) was added to the nitrogen purged solution and incubated for 2 hours. The prepared solution was treated with 95% ethanol (3 volumes) to precipitate aqueous soluble Cs [12]. It was redissolved in deionised water and dialysed (using 12-kDa cutoff dialysis membrane, Sigma Chemical Co., MO, USA) overnight. The obtained solution was lyophilised (Virtis, Gardiner, NY, USA) and stored at 4°C for further use.

2.2.2 Optimisation of synthesis of Cs placebo nanocapsules: The Cs placebo nanocapsules were prepared following the ionic gelation method explained by Calvo *et al.* [25].

Table 1 Different concentration combinations of Cs and TPP

Formulation code	Conc. of Cs, mg/ml	Conc. of TPP, mg/ml
C1	1.0	1.0
C2	1.0	1.5
C3	1.0	2.0
C4	1.5	1.0
C5	1.5	1.5
C6	1.5	2.0
C7	2.0	1.0
C8	2.0	1.5
C9	2.0	2.0

Table 2 Different concentration combinations of PEG to Cs

Formulation code	Conc. of PEG, mg/ml
CP1	5
CP2	10
CP3	15
CP4	20

The nanocapsules were synthesised by the dropwise addition of the tripolyphosphate (TPP) (cross linking agent) dissolved in double distilled water to the aqueous solution of Cs. Nine combinations of three different concentrations of Cs and TPP were tried in triplicates (Table 1). The three different concentrations of Cs and TPP were selected based on the literature survey done in reference to Cs nanocapsules [25–27].

2.2.3 Optimisation of synthesis of PEG modified Cs placebo nanocapsules: The best combination of Cs placebo nanocapsules was modified with four different concentrations of PEG based on method described by Wu *et al.* [16]. Aqueous PEG solution was added in dropwise manner to the aqueous Cs – TPP solution under constant stirring. Four different concentrations of PEG were tried in combination with Cs – TPP (Table 2). In all the four formulations tried, the PEG concentration was taken in high content compared with that of Cs in order to obtain high profile distribution for better efficacy [17]. The PEG modified nanocapsules were conceived with the intention of making these nanocapsules more stable in physiological fluids and to achieve increased blood circulation time with lower recognition by the host immune system [28].

2.2.4 Optimisation of synthesis of TQ loaded PEG modified Cs nanoencapsules: Initially a stock solution of TQ was prepared. 50 mg of TQ was dissolved in a solution containing 10 ml of distilled water and 10 ml of ethanol (Salmani *et al.* [29] published TQ was more stable when dissolved in ethanol and water in ratio 1:1 than in other solvents). The concentration of the drug in the stock solution was 2.5 mg/ml. The required amount of drug was taken from this stock solution throughout the project.

The best combination of PEG modified Cs placebo nanocapsule was loaded with TQ. Four different ratios of drug to polymer (w/w) were tried (Table 3) to get the best combination of drug and polymer based on particle size, polydispersity index and encapsulation efficiency (EE). TQ dissolved in mixture of ethanol and water was added in drops to the Cs solution under constant stirring followed by the addition of PEG and TPP (Fig. 1).

2.2.5 Characterisation of nanoencapsules using dynamic light scattering (DLS) zeta-particle size analyser: The zeta potential and particle size of the synthesised nanocapsule was measured using DLS particle size analyser (Malvern Zeta sizer v 2.1, UK). Zeta potential analysis was observed in automatic mode using folded capillary cells. All DLS measurements were performed at 25.0 ± 0.1°C and at 90° scattering angle. Zeta potential measurements were reproduced minimum three times to reduce errors in measuring. The synthesised nanoencapsulated solution was sonicated before measuring. To avoid or reduce the errors in measuring the particle size, all the samples were prepared and analysed in triplicates. The mean and standard deviation were calculated using Graph Pad Instat software.

2.2.6 Characterisation of nanoencapsules using scanning electron microscope (SEM): The surface morphology analysis of the TQ loaded PEG modified Cs nanoencapsules was analysed using LEO-435-VP Electron Microscope (LEO Electron Microscopy Ltd,. UK) with an accelerating voltage of 20 keV. A drop of the nanoencapsulated TQ was dried in a cover slip, coated with Au and then observed.

2.2.7 Characterisation of nanoencapsules using atomic-force microscopy (AFM): 5 µl of sample was spread on a glass slide and dried at room temperature. The prepared sample was analysed in Park NX 20 (Korea) scanning probe microscope. Scanning was done in tapping mode using commercial silicon probes with cantilevers. Cantilevers with a length of 228 (resonance frequencies of 5–98 kHz, spring constants of 3.0–7.1 Nm with scan rate of 1 Hz) and 5 nm normal tip curvature radius were used for scanning the sample. A minimum of five images from sample was analysed to ensure its reproducibility.

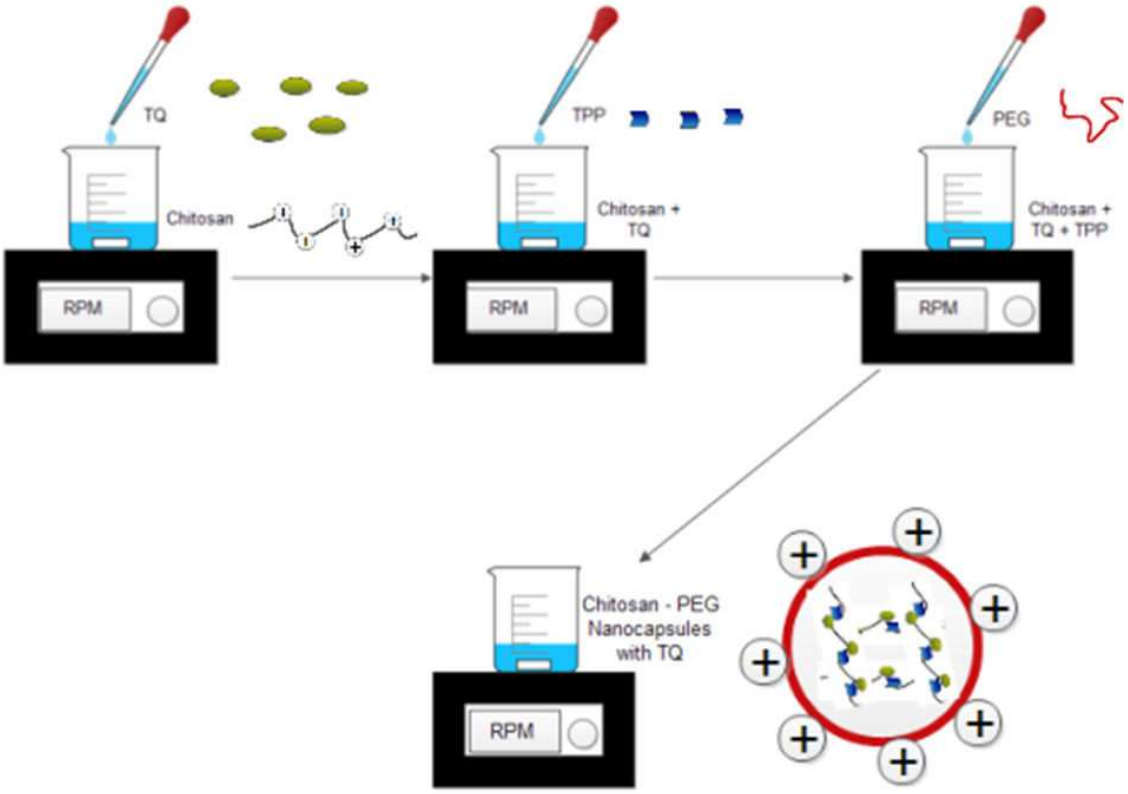

Fig. 1 *Schematic illustration of synthesis of chitosan – PEG nanocapsules loaded with TQ*

2.2.8 Characterisation of nanoencapsules using X-ray powder diffraction (XRD): X-ray diffractometry was performed for TQ, Cs PEG placebo nanocapsules and Cs PEG nanocapsules loaded with TQ to investigate the changes in phase or physical form of TQ caused in dispersion in the formulated nanocapsules. XRD patterns were recorded over the range 2θ from 2 to 50°C using an PANanalytical X'pert PRO XRD (PANalytical, Almelo, The Netherlands) with a scanning rate of 5°/minute.

2.2.9 Characterisation of nanoencapsules using Fourier transform-infrared (FTIR) spectroscopy: To study the possible interaction between Cs, PEG and TQ, the FTIR analysis was performed. 2–5 mg of Cs and PEG were separately mixed with KBr to form pellets using FW-4A pelletiser and analysed in FTIR (SCHIMADZU, IRAffinity1, Japan). The liquid sample TQ and TQ loaded nanoencapsules was analysed directly in FTIR (SCHIMADZU, MIRACLE 10, Japan).

2.2.10 Process yield (Y) and EE: The process yield of the placebo nanocapsules were calculated as per the following equation.

$$\text{Process yield (Y)} = \frac{W_1}{W_2} \times 100 \tag{1}$$

where W_1–Weight of dried nanocapsules recovered, W_2–Sum of initial dry weight of starting materials.

The placebo nanocapsules were centrifuged at 10,000 rpm, 4°C for 15 min. The pellet was separated from the supernatant. The pellet was air dried and then weighed.

Table 3 Different ratios of Cs and TQ

Formulation code	Polymer : drug ratio
CPT1	1:1
CPT2	1:2
CPT3	1:3
CPT4	1:4

The EE of the PEG modified Cs nanoencapsules loaded with TQ was calculated as per the following equation.

$$\text{Encapsulation efficiency (EE)} = \frac{(\text{Total drug} - \text{Free drug})}{\text{Total drug}} \times 100 \tag{2}$$

The nanoencapsulated TQ was centrifuged at 15,000 rpm, 4°C for 30 min. The amount of free TQ in the supernatant was dissolved in ethanol and sonicated for 10 min after which its absorbance at 330 nm was measured using UV Visible Spectrophotometer (UV-9000S, Lark, India) [15]. The amount of drug was estimated from the standard curve of TQ in ethanol. To avoid or reduce the errors in calculating the process yield and EE, all the samples were prepared and analysed in triplicates. The mean and standard deviation were calculated using Graph Pad Instat software.

2.2.11 Drug release studies: The release of drug from the PEG modified Cs nanoencapsules was studied using dialysis. The PEG modified nanoencapsules were dispersed in 5 ml of PBS (pH of 7.4) in a dialysis membrane (MWCO-12KDa, HiMedia, India) bag immersed in a beaker containing 80 ml PBS at pH of 7.4 under constant stirring. UV Visible spectrophotometer (UV-9000S, Lark, India) was used to calculate the concentration of TQ released from the dialysis bag at regular intervals. The absorbance for TQ was measured at 330 nm each time.

3 Results and discussion

3.1 Optimisation of Cs placebo nanocapsules

Among the nine formulations of Cs and TPP prepared, C6 (Cs 1.5 mg/ml and TPP 2 mg/ml) had minimum particle size of 127.03 nm, minimum PDI of 0.198 and maximum process yield of 34.5% (Table 4). Figs. 2*a* and *b* represents the particle size distribution of C6. From the particle size distribution graph obtained, it is evident that there is a wide distribution of particle size with the majority of particles within the size range of 100–150 nm. On visible analysis the formulation C6 was opalescent in nature. Whereas, C1 and C2 was clear without visible opalescence indicating the inadequacy of

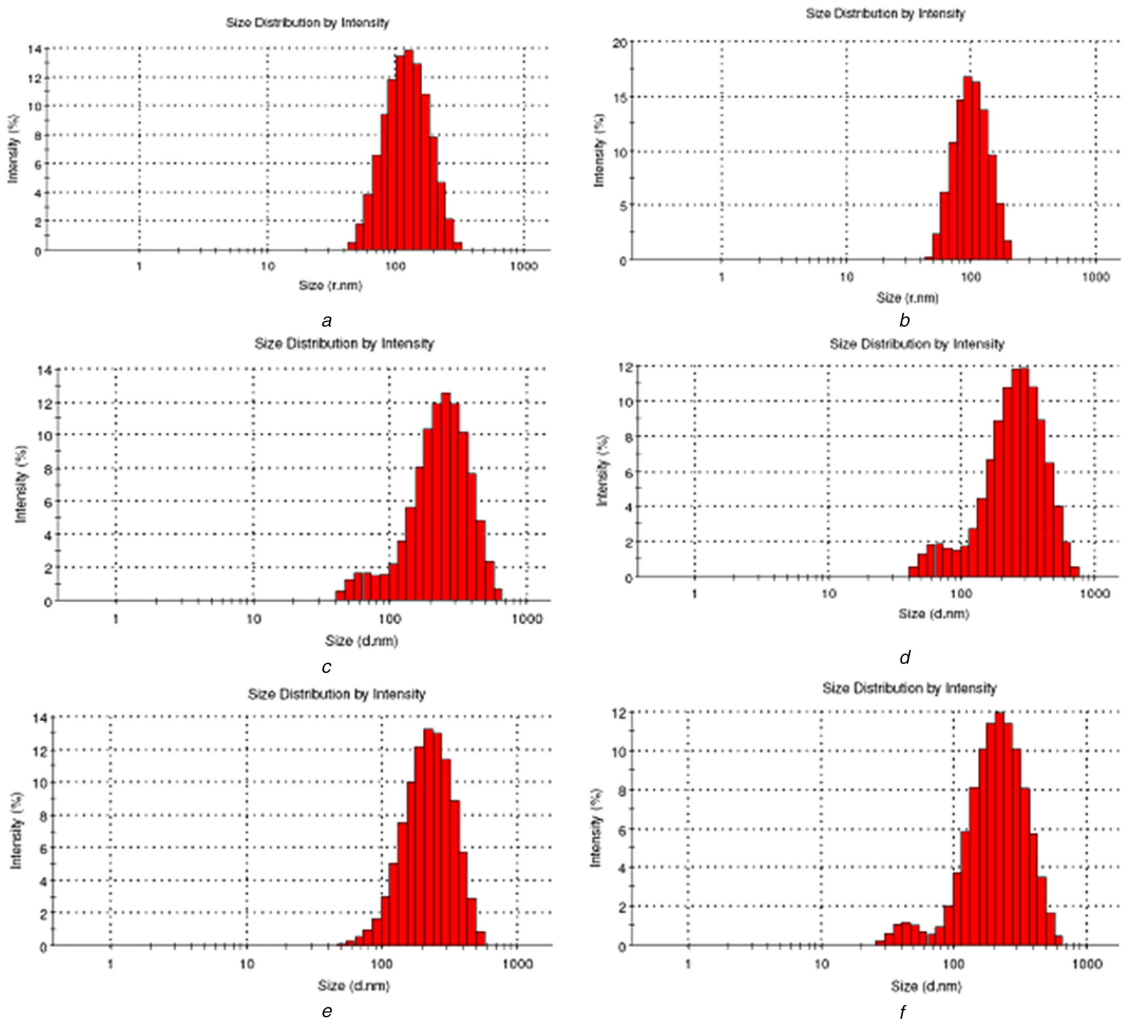

Fig. 2 *Particle size distribution graph*

(a) Particle size distribution of sample C6, ***(b)*** Particle size distribution of sample C6 (duplicate), ***(c)*** Particle size distribution of sample CP2, ***(d)*** Particle size distribution of sample CP2 (duplicate), ***(e)*** Particle size distribution of sample CPT2, ***(f)*** Particle size distribution of sample CPT2 (duplicate)

Cs – Tpp ratio that would lead to the formation of cross linked structure of Cs. This inadequacy has led to larger particle size in these formulations. However smaller particle size was noted for C3 (compared with C1 and C2) with milky in appearance. In the first three combinations, the process yield calculated using (1) was higher for the combination containing higher TPP concentration. C4 and C5 resulted in larger particle size and lower process yield than C6, though their appearance was similar to that of C6 (opalescence). As Cs concentration increases Cs molecules would approach each other with a limit, leading to a limited increase in intermolecular cross-linking, thus larger nanoscale particles are formed in formulation C7, C8 and C9. In this last three combinations (C7, C8, C9) the process yield was higher for the combination containing higher TPP concentration similar to the first three combinations (C1, C2 and C3) and the next three combinations (C4, C5 and C6). Alam *et al.* [27] on developing a Cs nanocapsule loaded with drug for nose to brain targeting obtained similar results. Fan *et al.* [30] described that even at a low mass ratio of Cs to TPP, stable nanoparticles can be formed from Cs at low concentration, however Cs at higher concentration could only form stable nanoparticles at a higher mass ratio of Cs to TPP. The results of particle size analysis has thus indicated that higher concentration of TPP promotes more cross linking of Cs and TPP in the nanocapsules formation resulting in smaller sizes. Observing the process yield of all the nine combinations of Cs and TPP, it is evident that the process yield is higher when the concentration of TPP is higher than that of Cs. It may be due to the fact that more concentration of TPP enhances more and effective cross linking of Cs polymers resulting in the formation of more number of nanocapsules yielding higher process yield.

Table 4 Particle size, PDI and process yield of Cs placebo nanocapsules

Sample	Particle size (nm)Mean ± S.D.	Process yield (Y)Mean ± S.D.	PDIMean ± S.D.
C1	234.80 ± 13	16.50 ± 3.77	0.287 ± 0.05
C2	238.40 ± 17	17.53 ± 2.16	0.305 ± 0.03
C3	197.43 ± 07	28.67 ± 5.69	0.260 ± 0.02
C4	239.80 ± 07	8.70 ± 1.97	0.256 ± 0.03
C5	210.90 ± 09	28.53 ± 5.02	0.242 ± 0.02
C6	127.03 ± 19	34.50 ± 2.15	0.198 ± 0.04
C7	335.07 ± 13	10.03 ± 2.95	0.283 ± 0.07
C8	330.57 ± 17	19.70 ± 4.56	0.270 ± 0.06
C9	305.33 ± 13	24.33 ± 4.04	0.266 ± 0.02

3.2 Optimisation of PEG modified Cs placebo nanocapsules

Among the four combinations of PEG with Cs nanocapsules analysed for minimum particle size, minimum PDI and maximum process yield, CP2 with a particle size of 186.0 nm, PDI of 0.221 and process yield of 38.9% was the best one (Table 5). Figs. 2*c* and *d* represents the particle size distribution of the CP2. The particle size distribution graph of CP2 depicts wide distribution of particle size with the majority of particles within the size range of 100–200 nm. The increased particle size of these nanocapsules after the addition of PEG is a good indication of the incorporation of PEG in the previous nanocapsule structure. Zhang *et al.* [31] and Sheng *et al.* [18] have earlier reported similar or even larger size of PEG

modified Cs nanocapsules loaded with drugs. The larger size reported earlier is due to the drug loaded in the capsules. Few previously submitted studies on PEG modified Cs nanocapsules [18, 31, 32] describe that increase in the concentration of PEG would increase the particle size of the nanocapsules formed. The CP3 and CP4 (concentration of PEG 15 and 20 mg/ml, respectively) resulted in larger particles than CP 2 (concentration of PEG 10 mg/ml) in accordance to the results described in earlier studies mentioned above. However, the particle size of CP1 (concentration of PEG 5 mg/ml) was slightly greater than that of CP2 and this might be due to the higher profile distribution of CP2 formulation than that of CP1 due to the higher concentration of PEG. The minimum particle size and higher process yield of CP2 than CP1, CP3 and CP4, directs us to consider CP2 for further drug loading.

3.3 Optimisation of PEG modified Cs nanocapsules loaded with TQ

Four different ratios of drug to polymer (w/w) was analysed based on EE, particle size and PDI to obtain the best combination of drug and polymer. Among them, CPT2 with the particle size of 192.7 nm, PDI of 0.166 and EE of 68.32% was the best one (Table 6). Figs. 2*e* and *f* represents the particle size distribution of the CPT2 exhibiting a wide distribution of particle size with the majority of particles within the size range of 100–200 nm. More amount of drug gets loaded when there is more amount of drug added to lesser amount of polymer. This was earlier discussed by Abu-Dahab *et al.* [33] as he found that the ratio of TQ – Cyclodextrin at 1:0.25 formed distinguishable homogenous nanoparticles and preserved the antiproliferative activity of TQ effectively. His discussion coincides with the results obtained in this work. Particle size of Cs- PEG nanocapsules similar to the result obtained in this work or even larger was described earlier [18, 31]. From the results it can be inferred that the size of the nanoparticles is influenced by the amount of drug and polymer. EE calculated using (2) was found to be higher for CPT2 than CPT1, CPT3 and CPT4. EE of 68.32% obtained in the present work is higher than that of the EE reported by Alam *et al.* [27] while they encapsulated TQ using Cs. The comparison between the observed and the reported results clearly indicates that PEG modification of Cs has positive effects on EE along with the other advantages described earlier in introduction.

The final optimised sample (CPT2) was taken further for other physicochemical characterisation and drug release studies.

3.4 Zeta potential analysis

The nanocapsule surface charge and the physical stability of polymeric nanocapsule developed was studied using zeta potential. High positive zeta potential preferably indicates good stability of nanocapsule developed [34]. The zeta potential of PEG modified chitosan nanocapsule developed was 48 mV indicating very good stability (Fig. 3*h*). Larsson *et al.* has previously reported carboxy methyl hexanoyl Chitosan with the similar zeta potential value exhibiting good stability as a protein carrier.

Table 5 Particle size, PDI and process yield of PEG modified Cs placebo nanocapsules

Sample	Particle size (nm)Mean ± S.D.	Process yield (Y)Mean ± S.D.	PDIMean ± S.D.
CP1	203.6 ± 19.86	30.00 ± 1.28	0.234 ± 0.006
CP2	186.0 ± 10.51	38.9 ± 0.30	0.221 ± 0.013
CP3	205.7 ± 11.9	24.63 ± 2.12	0.245 ± 0.011
CP4	201.2 ± 3.0	28.46 ± 0.76	0.267 ± 0.008

Table 6 Particle size, PDI and EE of PEG modified Cs nanocapsules loaded with TQ

Sample	Particle size (nm)Mean ± S.D.	PDIMean ± S.D.	Encapsulation efficiency %Mean ± S.D.
CPT1	196.40 ± 15.25	0.192 ± 0.07	42.47 ± 1.01
CPT2	192.70 ± 5.30	0.166 ± 0.04	68.32 ± 2.74
CPT3	206.10 ± 19.16	0.204 ± 0.08	54.54 ± 1.98
CPT4	221.80 ± 15.55	0.212 ± 0.14	59.83 ± 2.34

3.5 Surface morphology analysis using SEM and AFM

The SEM photograph of the PEG modified Cs nanocapsules loaded with TQ revealed that the drug-loaded nanocapsules are spherical in shape. The surface texture of the nanocapsules was found to be smooth. Figs. 3*a* and *b* depicts the morphology of nanocapsules analysed at a magnification of 20,000×, Figs. 3*c* and *d* depicts the morphology of the nanocapsules analysed at a magnification of 50,000×. The size of the nanocapsules was measured and indicated in the image as they lie in the range between 100 to 300 nm. Bhattacharya *et al.* [15] published similar results on morphology of PEG nanocapsules with smooth surface and spherical structure. Aggregation of nanocapsules was because of the air drying of the sample over the cover slip. The size of the nanocapsules observed in SEM was similar to that of particle size obtained in particle size analyser.

The nanocapsule shape, structure and interparticle organisation were characterised using AFM. The nanocapsules prepared were spherical in shape. The three dimensional image of the sample depicted heterogenous distribution in size and height of nanocapsules (Fig. 3*e*). The top view of height image of the sample shows rough surface of the sample (Fig. 3*f*). The horizontal and the lateral features of the surface were observed using the space parameters (Fig. 3*g*).

3.6 XRD analysis

XRD analysis was performed to investigate the characteristics of TQ inside Cs PEG nanocapsules (Figs. 4*a–c*). The absence of crystalline peak of chitosan in the Cs PEG placebo nanocapsules revealed the conformational transformation of chitosan from semi-crystalline to amorphous due to its ionic gelation with negatively charged particles [10]. The disappearance of crystalline peak of TQ in the Cs PEG nanocapsules loaded with TQ confirmed the molecular dispersion of TQ within the Cs PEG nanocapsules [27].

3.7 FTIR analysis

FTIR spectra of Cs, PEG, TQ and PEG modified Cs nanoencapsules loaded with TQ is shown in Figs. 5*a–d*, respectively. FTIR spectra of Cs (Fig. 5*a*) showed its characteristic peak 3448.2 cm^{-1} which indicated the presence of alcohols and phenols (O-H stretching vibrations). The peak obtained in 2924.09 in the same spectrum corresponds to the valence vibrations of C–H bonds in methylene groups. The symmetric deformation vibrations of amino group are represented by the band at 1381.03 cm^{-1}. Peaks between the ranges of 1430–1370 cm^{-1} (C) are due to the deformation vibrations of –CH2– and -OH groups. FTIR spectrum of pure PEG (Fig. 5*b*) showed distinct peaks in the range between 1000–1400 cm^{-1} (1032.46, 1280.73, 1103.28 cm^{-1}), 956.69 and 840.96 cm^{-1}. Deygen and Kudryashova [35] have described similar regions of characteristic peaks for the FTIR spectrum of Cs and PEG as they studied the structure and stability of anionic liposome complexes with PEG – Cs branched co polymer. Characteristic peak of TQ as described earlier by Cardoso *et al.* [36] was found in wavelength 1743.65 cm^{-1} (Fig. 5*c*), which indicated the presence C=O stretch (carbonyl group). The FTIR spectrum of PEG modified Cs nanocapsules loaded with TQ (Fig. 5*d*) depicts that PEG modification of Cs results in the appearance of a band at 1041 cm^{-1} (valence vibrations of the C–O–C bond). It is also one of the characteristic peak range of the PEG molecule. The chitosan band at 1200–950 cm^{-1} contributes little to the total intensity at 1041 cm^{-1} in this spectrum as its intensity is less than the C–O–C band. The observed difference in the intensity of the band in the PEG modified Cs nanocapsules loaded with TQ spectrum compared with Cs indicates the modification of Cs using

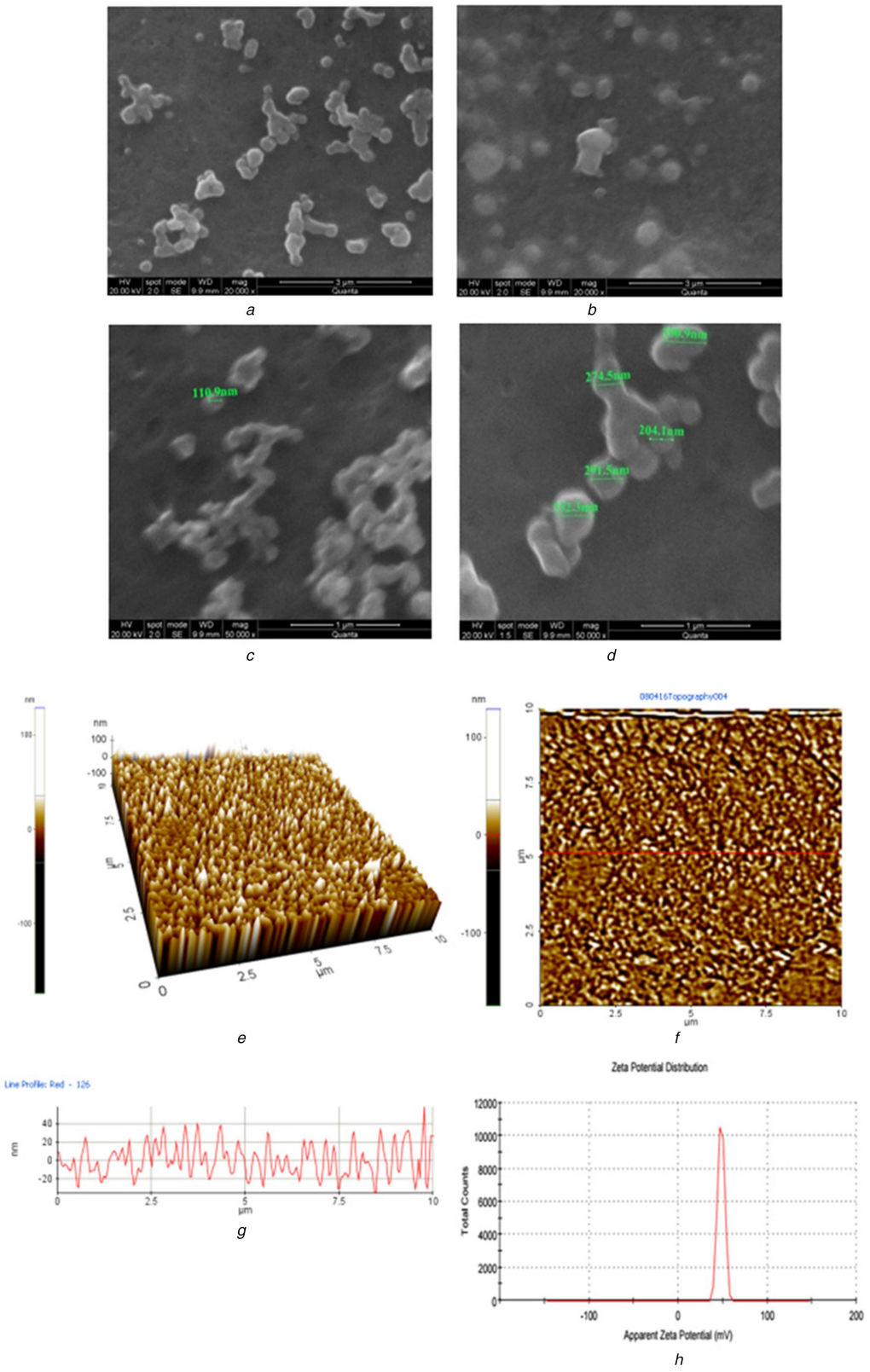

Fig. 3 *SEM photograph of PEG modified CS TPP nanocapsules loaded with TQ*

(a) SEM photograph of PEG modified Cs nanocapsules loaded with TQ at a magnification of 20,000x, ***(b)*** SEM photograph of PEG modified Cs nanocapsules loaded with TQ at a magnification of 20,000x, ***(c)*** SEM photograph of PEG modified Cs nanocapsules loaded with TQ at a magnification of 50,000x, ***(d)*** SEM photograph of PEG modified Cs nanocapsules loaded with TQ at a magnification of 50,000x, ***(e)*** 3D AFM image of height of Cs-PEG nanocapsuless loaded with TQ, ***(f)*** AFM image (Top view) of height of Cs-PEG nanocapsules loaded with TQ, ***(g)*** AFM image (Line profile) of height of Cs-PEG nanocapsules loaded with TQ, ***(h)*** Zeta potential of Cs-PEG nanocapsules loaded with TQ

PEG. Wu *et al.* [16] and Deygen and Kudryashova [35] have explained similar results using FTIR for the PEG modification of Cs. Important fact to be noted is that the characteristic peak of the TQ is also found in the FTIR spectrum of PEG modified Cs nanocapsule, indicating there is no chemical changes in TQ after encapsulation, while the characteristic peaks of Cs and PEG have undergone variations in the FTIR spectrum of PEG modified Cs nanocapsules confirming the interaction occurred between them during encapsulation.

These results confirm the presence of Cs, PEG and TQ in the PEG modified Cs nanocapsules loaded with TQ prepared and also the interaction between them.

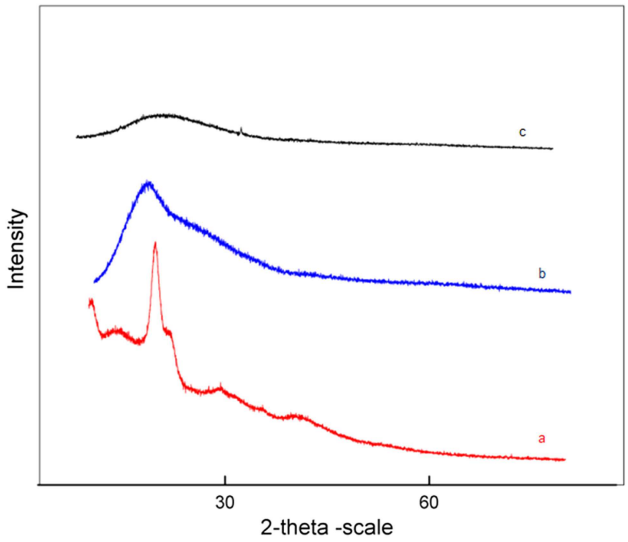

Fig. 4 *X-ray diffraction profiles*
(a) X-ray diffraction spectroscopy of TQ, ***(b)*** X-ray diffraction spectroscopy Cs PEG placebo Nps and, ***(c)*** X-ray diffraction spectroscopy Cs PEG nanocapsules with TQ

3.8 In vitro drug release

The release profile of TQ from PEG modified Cs nanoencapsules showed sustained release of TQ from the nanopolymer at pH of 7.4 in phosphate buffer. Characteristic slow-release pattern through a span of 72 h was observed for the released TQ from the PEG modified Cs nanocapsules. Initially there was a slow release followed by gradual increase. The rapid initial burst release of the drug was not found because the TQ embedded in the surface of the polymeric nanocapsules were washed by centrifugation before subjecting it to the dialysis membrane. The controlled-release profile of TQ-Nps is shown in Fig. 6. This slow and sustained release of TQ from the PEG modified Cs nanocapsules exhibit better results than other polymeric nanocapsules used to encapsulate TQ. The UV absorbance spectrum of TQ released from polymer even after 48 h showed that the TQ was stable inside the polymer. Earlier Nallamuthu *et al.* [5] studied and described about the burst release of TQ from TQ loaded PLGA nanocapsules in initial 10 hours period and thereafter followed by sustained release of TQ. The difference in release from this study may be due to nature of different polymers used (PLGA is a synthetic polymer soluble in solvents other than water while Cs used in this study is aqueous soluble)

4 Conclusion

Cs placebo nanocapsules were successfully synthesised and it showed excellent compatibility for association with PEG. PEG modified Cs nanocapsules were synthesised and the synthesised nanocapsules were characterised using DLS Zetasizer, SEM, AFM, XRD and FTIR. PEG interaction with Cs is through the intermolecular hydrogen bonding between the electronegative oxygen atom of PEG and electropositive amino hydrogen Cs. TQ was successfully encapsulated within PEGylated Cs nanocapsules and the release profile of TQ from PEG modified Cs nanocapsules had a slow and sustained release. This primary study on the PEG modified Cs nanocapsules loaded with TQ throws light on the advantages of using PEG modified capsules as a drug carrier to deliver TQ. The obtained primary results urge us to take forward this research further to investigate the stability and bioavailability of TQ in the nanocapsule through *in-vitro* and *in-vivo* studies and finally study its effect on inflammatory disorders to develop a product for clinical application.

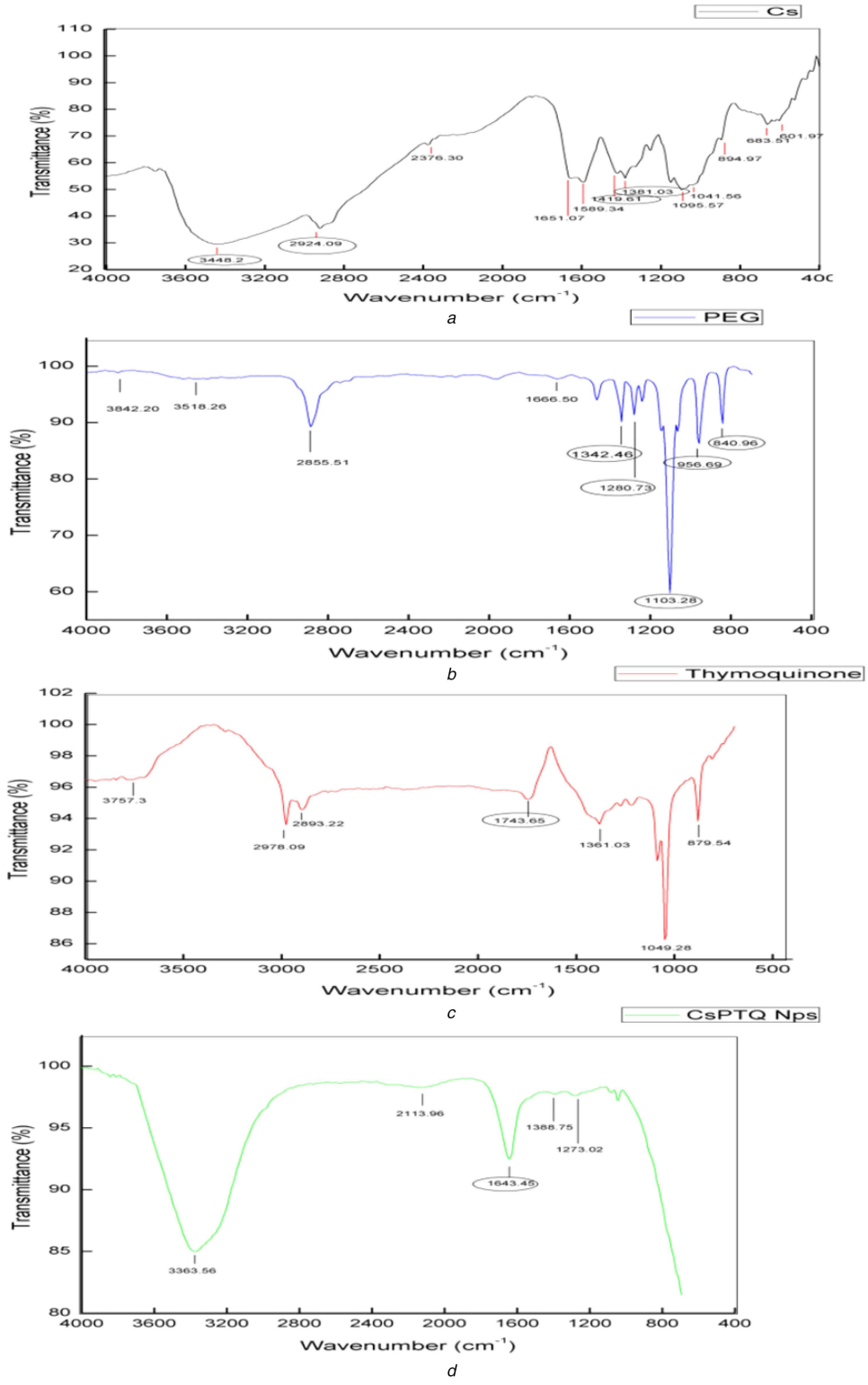

Fig. 5 *FTIR spectral analysis*

(a) FTIR spectrum of Cs, ***(b)*** FTIR spectrum of PEG, ***(c)*** FTIR spectrum of TQ, ***(d)*** FTIR spectrum of PEG modified Cs nanocapsules loaded with TQ

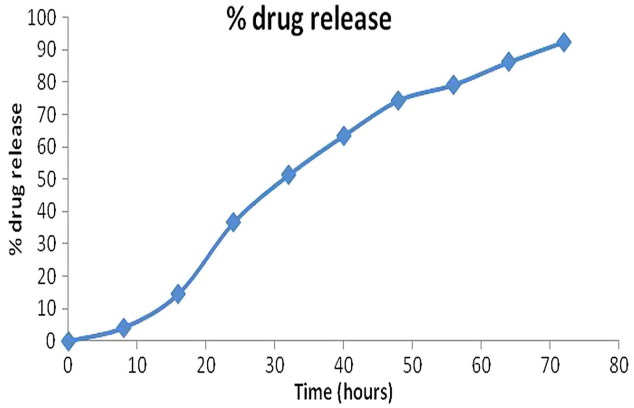

Fig. 6 *TQ release in PBS (pH 7.4, 37°C) from PEG modified Cs nanocapsules loaded with TQ*

5 References

[1] Naz, H.: '*Nigella sativa*: the miraculous herb', *Pak. J. Biochem. Mol. Biol*, 2011, **44**, (1), pp. 44–48

[2] Paarakh, P.M.: '*Nigella sativa* Linn. – A comprehensive review', *Indian J. Nat. Prod. Res.*, 2010, **1**, (4), pp. 409–429

[3] D'Antuono, F.L., Moretti, A., Lovato, A.F.S.: 'Seed yield, yield components, oil content and essential oil content and composition of *Nigella satiaiva* L. and *Nigella damascena* L', *Ind. Crops Prod.*, 2002, **15**, pp. 59–69

[4] Raschi, A.B., Romano, E., Benavente, A.M., *et al.*: 'Structural and vibrational analysis of thymoquinone', *Spectrochim. Acta*, 2010, Part A 77, pp. 497–505

[5] Nallamuthu, I., Parthasarathi, A., Khanum, F.: 'Thymoquinone-loaded PLGA nanoparticles: antioxidant and anti-microbial properties', *Int. Current Pharm. J.*, 2013, **2**, (12), pp. 202–207

[6] Schneider-Stock, R., Fakhoury, I.H., Zaki, A.M., *et al.*: 'Thymoquinone: fifty years of success in the battle against cancer models', *Drug Discov. Today*, 2014, **19**, (1), pp. 18–30

[7] El-Khouly, D., El-Bakly, W.M., Awad, A.S., *et al.*: 'Thymoquinone blocks lung injury and fibrosis by attenuating bleomycin-inducedoxidative stress and activation of nuclear factor Kappa-B in rats', *Toxicology*, 2012, **302**, pp. 106–113

[8] Tembhurne, S.V., Feroz, S., More, B.H., *et al.*: 'A review on therapeutic potential of *Nigella sativa* (kalonji) seeds', *J. Med. Plants Res.*, 2014, **8**, (3), pp. 167–177

[9] Riva, R., Ragelle, H., des Rieux, A., *et al.*: 'Chitosan and chitosan derivatives in drug delivery and tissue engineering', in Jayakumar, R., Prabaharan, M., Muzarelli, M.A.A. (Eds): '*Adv Polym Sci*' (Springer Berlin Heidelberg, 2011), pp. 19–44

[10] Agrawal, S., Ahmad, H., Dwivedi, M., *et al.*: 'PEGylated chitosan nanoparticles potentiate repurposing of ormeloxifene in breast cancer therapy', *Nanomedicine*, 2016, **11**, (16), pp. 2147–2169

[11] Unsoy, G., Yalcin, S., Khodadust, R., *et al.*: 'Synthesis optimization and characterization of chitosan-coated ironoxide nanoparticles produced for biomedical applications', *J. Nanoparticle Res.*, 2012, **14**, (11), pp. 1–13

[12] Arunkumar, R., Prashanth, K.V.H., Baskaran, V.: 'Promising interaction between nanoencapsulated lutein with low molecular weight chitosan: characterization and bioavailability of lutein in vitro and in vivo', *Food Chem.*, 2013, **141**, (1), pp. 327–337

[13] Chun, W., Xiong, F., Sheng, L.: 'Water soluble chitosan nanoparticles as a novel carrier system for protein delivery', *Chin. Sci. Bull.*, 2007, **52**, (7), pp. 883–889

[14] Tang, Z.-X., Qian, J.-Q., Shi, L.-E.: 'Preparation of chitosan nanocapsules as carrier for immobilized enzyme', *Appl. Biochem. Biotechnol.*, 2007, **136**, pp. 77–96

[15] Bhattacharya, S., Ahir, M., Patra, P., *et al.*: 'PEGylated-thymoquinone-nanoparticle mediated retardation of breast cancer cell migration by deregulation of cytoskeletal actin polymerization through miR-34a', *Biomaterials*, 2015, **51**, pp. 91–107

[16] Wu, Y., Yang, W., Wang, C., *et al.*: 'Chitosan nanoparticles as a novel delivery system for ammonium glycyrrhizinate', *Int. J. Pharm.*, 2005, **295**, pp. 235–245

[17] Lollo, G., Hervella, P., Calvo, P., *et al.*: 'Enhanced in vivo therapeutic efficacy of plitidepsin-loaded nanocapsules decorated with a new poly-aminoacid-PEG derivative', *Int. J. Pharm.*, 2015, **483**, (1), pp. 212–219

[18] Sheng, Y., Liu, C., Yuan, Y., *et al.*: 'Long-circulating polymeric nanoparticles bearing a combinatorial coating of PEG and water-soluble chitosan', *Biomaterials*, 2009, **30**, (12), pp. 2340–2348

[19] Guo, F., Fan, Z., Yang, J., *et al.*: 'A comparative evaluation of hydroxycamptothecin drug nanorods with and without methotrexate prodrug functionalization for drug delivery', *Nanoscale Res. Lett.*, 2016, **11**, p. 384

[20] Mahapatro, A., Singh, D.K.: 'Biodegradable nanoparticles are excellent vehicle for site directed in-vivo delivery of drugs and vaccines', *J. Nanobiotechnol.*, 2011, **9**, pp. 1–11

[21] Jia, M., Li, Y., Yang, X., *et al.*: 'Development of both methotrexate and mitomycin C loaded PEGylated chitosan nanoparticles for targeted drug delivery and synergistic anticancer effect', *ACS Appl. Mater. Interfaces*, 2014, **6**, (14), pp. 11413–11423

[22] Luo, F., Li, Y., Jia, M., *et al.*: 'Validation of a Janus role of methotrexate – based PEGylated chitosan nanoparticles in vitro', *Nanoscale Res. Lett.*, 2014, **9**, (1), pp. 1–13

[23] Lin, J., Li, Y., Li, Y., *et al.*: 'Drug/dye-loaded, multifunctional PEG-chitosan-iron oxide nanocomposites for methotrexate synergistically self-targeted cancer therapy and dual model imaging', *ACS Appl. Mater. Interfaces*, 2015, **7**, (22), pp. 11908–11920

[24] Hou, Z., Lin, J., Li, Y., *et al.*: 'Validation of a dual role of methotrexate based chitosan nanoparticles in vivo', *RSC Adv.*, 2015, **5**, p.41393

[25] Calvo, P., Remunan-Lopez, C., Vila-Jato, J.L., *et al.*: 'Novel hydrophilic chitosan-polyethylene oxide nanoparticles as protein carriers', *J. Appl. Polym. Sci.*, 1997, **63**, (1), pp. 125–132

[26] Zhang, H.L., Wu, S.H., Tao, Y., *et al.*: ' Preparation and characterization of water-soluble chitosan nanoparticles as protein delivery system', *J. Nanomaterials*, 2010, **1**, pp. 1–5

[27] Alam, S., Khan, Z.I., Mustafa, G., *et al.*: 'Development and evaluation of thymoquinone-encapsulated chitosan nanoparticles for nose-to-brain targeting: a pharmacoscintigraphic study', *Int. J. Nanomedicine*, 2012, **7**, pp. 5705–5718

[28] Andrade, F., Goycoolea, F., Chiappetta, D.A., *et al.*: 'Chitosan-Grafted copolymers and chitosan- ligand conjugates as matrices for pulmonary drug delivery', *Int. J. Carbohydr. Chem.*, 2011, **2011**, pp. 1–14

[29] Salmani, J.M.M., Asghar, S., Lv, H., *et al.*: 'Aqueous solubility and degradation kinetics of the phytochemical anticancer thymoquinone; probing the effects of solvents, pH and light', *Molecules*, 2014, **19**, (5), pp. 5925–5939

[30] Fan, W., Yan, W., Xu, Z., *et al.*: 'Formation mechanism of monodisperse, low molecular weight chitosan nanoparticles by ionic gelation technique', *Colloids Surfaces B Biointerfaces*, 2012, **90**, pp. 21–27

[31] Zhang, X., Zhang, H., Wu, Z., *et al.*: 'Nasal absorption enhancement of insulin using PEG-grafted chitosan nanoparticles', *Eur. J. Pharm. Biopharm.*, 2008, **68**, (3), pp. 526–534

[32] Zhu, S., Qian, F., Zhang, Y., *et al.*: 'Synthesis and characterization of PEG modified N-trimethylaminoethylmethacrylate chitosan nanoparticles', *Eur. Polym. J.*, 2007, **43**, (6), pp. 2244–2253

[33] Abu-Dahab, R., Odeh, F., Ismail, S.I., *et al.*: 'Preparation, characterization and antiproliferative activity of thymoquinone-β-cyclodextrin self assembling nanoparticles', *Die Pharmazie-An Int. J. Pharm. Sci.*, 2013, **68**, (12), pp. 939–944

[34] Larsson, M., Borde, A., Mattisson, E., *et al.*: 'Evaluation of carboxymethyl-hexanoyl chitosan as a protein nanocarrier', *Nanomaterials Nanotechnol.*, 2013, **1**, (3), pp. 3–7

[35] Deygen, I.M., Kudryashova, E.V.: 'Structure and stability of anionic liposomes complexes with PEG-chitosan branched copolymer', *Russ. J. Bioorg. Chem.*, 2014, **40**, (5), pp. 547–557

[36] Cardoso, T., Galhano, C.I.C., Ferreira Marques, M.F., *et al.*: 'Thymoquinone β-Cyclodextrin nanoparticles system: a preliminary study', *Spectrosc. Int. J.*, 2012, **27**, (5–6), pp. 329–336